Transition Met Chem (2011) 36:395–402
DOI 10.1007/s11243-011-9482-2

Synthesis, crystal structure, and DNA cleavage activity of a dinuclear nickel(II) complex with a macrocyclic ligand

Hong Hu · Yunfeng Chen · Hong Zhou · Zhiquan Pan

Received: 23 November 2010 / Accepted: 10 March 2011 / Published online: 25 March 2011

Abstract A new Ni(II) complex, namely $[Ni_2(OAc)L]\cdot ClO_4\cdot H_2O$, was synthesized by [2 + 2] cyclo-condensation between 2,6-diformyl-4-methylphenol and *N*,*N*-bis(3-aminopropyl)-4-methoxybenzylamine (amba) in the presence of nickel(II) and characterized by spectroscopy, elemental analysis, and X-ray single crystal diffraction. The interactions of the complex with DNA have been measured by spectroscopy and viscosity measurements. Absorption spectroscopic investigation reveals intercalative binding of the Ni(II) complex with DNA, with a binding constant of 2.6×10^4 M^{-1}. Fluorescence spectroscopy shows that the Ni(II) complex can displace ethidium bromide and bind to DNA, with a quenching constant of 7.57×10^3 M^{-1}. The appearance of increased CD bands near 245 and 275 nm gives evidence for effective complex DNA binding. The agarose gel electrophoresis studies show that the complex displays effective DNA cleavage activity in the absence of any external agents.

Introduction

The development of artificial metallonucleases as cellular regulators of DNA is of current interest in the fields of therapeutic and biochemical technology [1–3]. The search for artificial metallonucleases that can cleave DNA hydrolytically is a particular challenge because of the long intrinsic half-life for hydrolysis of DNA at pH 7 and 25 °C [4, 5]. Complexes of macrocyclic polyamines with two phenol groups have good nuclease activities because of their good ability to bind and cleave DNA. Thus, Shiping Yan and co-workers have demonstrated that macrocyclic Cu and Zn complexes with two phenol groups display efficient binding to calf thymus DNA (CT-DNA) and chemical nuclease activity in the presence of a reducing agent [6]. Kandaswamy and co-workers have synthesized a series of binuclear copper(II) complexes of macrocyclic polyamine ligands with two phenol groups, and they found that this kind of complex binds to DNA in an intercalative mode [7]. In contrast, the nickel(II) complexes of macrocyclic polyamines with two phenol groups have received much less attention. In fact, nickel(II) complexes with macrocyclic ligands were also found to have potential DNA cleavage reactivity [8]. In this paper, we report the synthesis of a new nickel(II) complex of a polyamine macrocyclic ligand with two phenol groups by template synthesis, as shown in Scheme 1. This complex is shown to have an efficient DNA-binding activity. The plasmid pBR322 DNA cleavage activity of the complex was investigated via agarose gel electrophoresis, and a possible mechanism for the cleavage process is also suggested.

Experimental

All chemicals were purchased from commercial sources and used as received. Solvents were dried according to standard procedures and distilled prior to use. 2,6-Diformyl-4-methylphenol was synthesized according to a procedure

Electronic supplementary material The online version of this article (doi:10.1007/s11243-011-9482-2) contains supplementary material, which is available to authorized users.

H. Hu · Y. Chen · H. Zhou · Z. Pan (✉)
Key Laboratory for Green Chemical Process of Ministry of Education, Wuhan Institute of Technology, 430073 Wuhan, People's Republic of China
e-mail: zhiqpan@163.com

Z. Pan
State Key Laboratory of Coordination Chemistry, Nanjing University, 210093 Nanjing, People's Republic of China

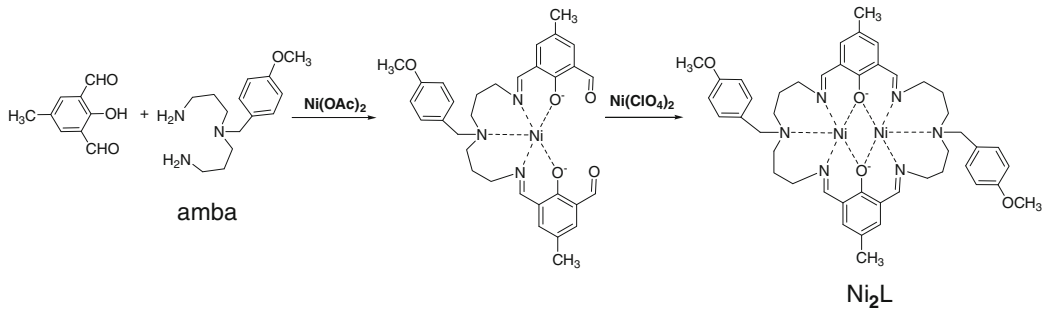

Scheme 1 Synthetic route for the preparation of Ni_2L. Both steps involve template synthesis with Ni^{2+} salts plus amba. The acetate ligand in the final complex is omitted for clarity

reported previously [9]. 4-Methoxybenzylamine and nickel(II) perchlorate hexahydrate were purchased from Alfa Aesar. Tris(hydroxymethyl)amino-methane (Tris), bromophenol blue, ethidium bromide (EB), agarose gel, and plasmid pBR322 DNA were purchased from Toyobo Co.

IR spectra were measured using KBr disks on a vector 22 FIIR spectrophotometer. ^{1}H NMR spectra were recorded on a Varian Mercury VX-300 spectrometer at 30 °C in D_2O with TMS as the internal reference. Elemental analyses were obtained on a Perkin-Elmer 240 analyzer. Electrospray mass spectra (ES–MS) were determined on a Finnigan LCQ ES-MS mass spectrograph using methanol as the mobile phase with an approximate concentration of 1.0 mmol dm^{-3}. Absorption spectra in the 190–700 nm range were recorded on a Shimadzu UV-2450 spectrophotometer. Circular dichroic spectra of DNA were obtained using a Jasco J-810 spectropolarimeter. Fluorescence spectra were recorded on a Jasco FP-6500 spectrophotometer. Cyclic voltammograms were run on a CHI model 750 B electrochemical analyzer in DMF solutions containing tetra(*n*-butyl)ammonium perchlorate (TBAP) as the supporting electrolyte. A three-electrode cell was used, which was equipped with a glassy carbon-working electrode, a platinum wire as the counter electrode and a Ag/AgCl electrode as the reference electrode. Scanning rates were in the range of 20–200 mV s^{-1}. The solution was deaerated for 15 min before measurements.

Preparation of the *N*,*N*-bis(2-cyanoethyl)-4-methoxybenzylamine (cmba)

Cmba was synthesized by an improved literature method [10]. To a solution of 4-methoxybenzylamine (13.7 g, 0.1 mol) in water (100 mL), acrylonitrile (16.0 g, 0.3 mol) was added dropwise at 0 °C, then the resulting mixture was refluxed for 90 h. After returning to room temperature, the mixture was extracted with dichloromethane, and the organic layer was washed with brine and dried with anhydrous sodium sulfate. After filtration, the solvent was removed to give the product as a yellow oil. Yield: 23.5 g (97%). The oil was used for the following reaction without further purification.

Preparation of the *N*,*N*-bis(3-aminopropyl)-4-methoxybenzylamine (amba)

A mixture of cmba (23.5 g, 0.097 mol) in methanol (200 mL) and active Raney-Ni (10.0 g) was vigorously stirred, and a solution of $NaBH_4$ (11 g, 0.291 mol) in 8 mol/L NaOH (70 mL) was added at such a rate as to maintain the temperature at 60 °C. After the addition was complete, the reaction mixture was stirred at room temperature overnight. The Raney-Ni catalyst was then removed by filtration, and the solvent was removed under reduced pressure. The crude amba was extracted with dichloromethane and dried with anhydrous sodium sulfate. After filtration, the solvent was distilled off to obtain the crude product as a colorless oil. Yield: 21.5 g (88%).

Amba·3HCl was prepared by acidifying amba with an HCl–EtOH solution, and the white precipitate was obtained. The precipitate was washed with EtOH several times and dried in vacuo. The pure product was obtained as its trihydrochloride by recrystallization from a minimum of water and ethanol [11]. Yield: 26.5 g (86%). Anal. Calc. for $C_{14}H_{28}ON_3Cl_3$: C, 46.6; H, 7.8; N, 11.7. Found: C, 46.5; H, 7.8; N, 11.6. IR (KBr, cm^{-1}): 3051, 2913 (C–H), 3359 (N–H), 1247, 1032 (C–O). ^{1}H NMR(D_2O, δ/ppm): 7.13 (d, 2H, 2ArH), 6.83 (d, 2H, 2ArH), 3.67 (s, 3H, –O–CH_3), 3.38 (s, 2H, Ar–CH_2), 2.45 (t, 4H, 2CH_2–NH_2), 2.28 (t, 4H, 2 N–CH_2), 1.51 (m, 4H, 2–CH_2–).

Preparation of $[Ni_2(OAc)L]ClO_4 \cdot H_2O$

Amba·3HCl (0.18 g, 0.5 mmol) was dissolved in H_2O (10 mL) and neutralized with NaOH (0.06 g, 1.5 mmol); the solution was added to a mixture of 2,6-diformyl-4-methylphenol (0.082 g, 0.5 mmol) and $Ni(OAc)_2 \cdot 4H_2O$ (0.124 g, 0.5 mmol) in ethanol (10 mL). The mixture was stirred overnight, and then $NaClO_4 \cdot H_2O$ (0.07 g,

0.5 mmol) in ethanol (10 mL) was added. After stirring for another 6 h, a yellow precipitate was collected. Green single crystals suitable for X-ray structure analysis were obtained by evaporation of an acetonitrile solution of complex. Yield: 0.12 g (46%). Anal. Calc. for $C_{48}H_{61}O_{11}N_6Ni_2Cl$: C, 54.8; H, 5.8; N, 8.0. Found: C, 54.7; H, 5.9; N, 8.0. IR (KBr, cm^{-1}): 3051, 2913 (C–H), 1642(C = N), 1081, 624 (ClO_4^{-1}), 1247, 1032 (C–O).

Determination of the crystal structure

Diffraction intensity data were collected on a SMART CCD area-detector diffractometer at 291 K using graphite monochromatic Mo Kα radiation ($\lambda = 0.71073$ Å). Data reduction and cell refinement were performed with the SMART and SAINT programs [12]. The structure was solved by direct methods (Bruker SHELXTL) and refined on F^2 by full-matrix least squares (Bruker SHELXTL) using all unique data [13]. All non-hydrogen atoms were refined anisotropically, and hydrogen atoms were refined on calculated positions using a riding mode.

DNA-binding experiments

CT-DNA (20 mg) was dissolved in Tris–HCl buffer (100 mL, 50 mM Tris–HCl, 50 mM NaCl, pH = 7.2) and kept at 4 °C for less than 4 days. The absorption ratio A_{260}/A_{280} was within the range of 1.8–2.0. The DNA concentration was determined via absorption spectroscopy using the molar absorption coefficient of 6,600 M^{-1} cm^{-1} (260 nm) for CT-DNA [14].

The nickel(II) complex was dissolved in DMF at a concentration of 5.0×10^{-5} M. The UV absorption titrations were performed by keeping the concentration of the complex fixed while varying the DNA concentration. Complex-DNA solutions were allowed to incubate for 30 min at room temperature before measurements were made. Absorption spectra were recorded using cuvettes of 1 cm path length at room temperature. The intrinsic binding constant K_b was calculated according to Eq. 1 [15]:

$$\frac{[\mathrm{DNA}]}{(|\varepsilon_a - \varepsilon_f|)} = \frac{[\mathrm{DNA}]}{(|\varepsilon_b - \varepsilon_f|)} + \frac{1}{k(|\varepsilon_b - \varepsilon_f|)} \quad (1)$$

where ε_a, ε_f and ε_b are the molar extinction coefficients of solutions containing both complex and DNA, free complex, and the complex bound to DNA, respectively.

Fluorescence quenching experiments were performed by adding a solution of the complex (1.5 μL) to EB-bound CT-DNA solution (1.5 μL) at different concentrations (12.5–200 μM). All experiments were carried out using cuvettes of 1 cm path length at room temperature. Samples were excited at 520 nm, and emission was recorded at 450–750 nm.

Circular dichroism (CD) is a useful technique to assess whether nucleic acids undergo conformational changes after interacting with complexes [16]. CD spectra of CT-DNA were recorded in the absence and presence of the complex, from 320 to 220 nm at a speed of 300 nm/min. Data were recorded at an interval of 0.1 nm at room temperature, and a cuvette of 3 mL volume was adopted in this experiment.

Viscosity measurements were carried out using a capillary viscometer at a constant temperature (23.0 ± 0.1 °C). Flow times were measured with a digital stopwatch and each sample was measured three times, and then an average flow time was calculated. Data are presented as $(F/F_0)^{1/3}$ versus molar ratio of complex to DNA [17], where F is the viscosity of DNA in the presence of complex and F_0 is the viscosity of DNA in the absence of complex.

DNA cleavage experiments

The cleavage of pBR322 DNA by the complex was examined by gel electrophoresis experiments. Negative supercoiled pBR322 DNA (0.5 μL, 0.5 μg/μL) was treated with different concentrations of complex (1 μL) in Tris–HCl buffer (1 μL, 50 mM Tris–HCl, 50 mM NaCl, pH = 7.2). After mixing, the mixtures were incubated at 37 °C for 3 h. The reactions were quenched by the addition of sterile solution (1 μL, 0.25% bromophenol blue and 40% w/v sucrose). The samples were then analyzed by electrophoresis for 1 h at 80 V on agarose gel in TAE buffer (40 mM Tris-base, 40 mM acetic acid and 1 mM EDTA, pH = 7.4). The gel was stained with EB (1 μg/μL) for 0.5 h after electrophoresis and then photographed.

Results and discussion

A macrocyclic binuclear nickel(II) complex was synthesized by Schiff base condensation of 2,6-diformyl-4-methylphenol with amba·3HCl in the presence of $Ni(OAc)_2{\cdot}4H_2O$ and $NaClO_4{\cdot}H_2O$. The synthetic pathway to the complex is shown in Scheme 1. In the IR spectrum of the complex, the sharp C=N stretching vibration corresponding to the imine groups of the macrocyclic framework is observed at 1,642 cm^{-1}, indicating that a macrocyclic complex has been synthesized. In addition, strong bands at 1,081 and 624 cm^{-1} can be ascribed to the ClO_4^- anion.

The ES-MS spectrum of the nickel(II) complex in methanol solution (Supplementary data S1) is dominated by a peak at m/z 933.50, corresponding to $[Ni_2(OAc)L]^+$ ($C_{48}H_{59}O_6N_6Ni_2$, calc. 933.39). The other peaks in the ES–MS of the nickel(II) complex are not discussed, due to their

low abundance (<5%). The ES–MS spectrum shows that $[Ni_2(OAc)L]^+$ is stable in methanol solution.

Crystal structure of $[Ni_2(OAc)L]ClO_4 \cdot H_2O$

A perspective view of $[Ni_2(\mu\text{-OAc})L]ClO_4 \cdot H_2O$ is given in Fig. 1, together with the atom labeling scheme. Crystallographic data and details about the data collection are presented in Table 1, and selected bond lengths and angles relevant to the nickel(II) coordination spheres of the complex are listed in Table 2. The angle between the two benzene rings in each complex is 61.21°. Two 4-methoxyphenoethyl groups are situated in the same side of the convexity of the distorted macrocycle.

The nickel complex is composed of a $[Ni_2(\mu\text{-OAc})L]^+$cation, a perchlorate anion, and a H_2O molecule. The two Ni atoms reside in the N_3O_2 sites of the macrocycle L^{2-}. The remaining sites of the distorted octahedral nickel(II) atoms are coordinated by μ_2-OAc. The coordination environment of the two nickel(II) atoms is different to those of the complexes described in the literature [18, 19]. Each Ni^{2+} has a six-coordinated environment. Deviation of the Ni(1) and Ni(2) atoms from the mean plane, formed by O1, O2, N5, and N6 and by O1, O2, N2, and N3, are 0.069 and 0.049 Å, respectively. The dihedral angle between the planes is 27.3°. The basal bond distances around the Ni(1) atom are in the range of 2.223–2.053 Å, which are longer than those in the reported six-coordinate nickel(II) complex [20]. The apical bond distances are Ni(1)–N(1) = 2.115(4) and Ni(1)–O(3) = 2.069(3) Å, with the bond angle O(3)–Ni(1)–N(1) = 166.26(14)°. The bond distances around the Ni(2) atom are in the 2.232–2.053 Å range. The apical bond distances are Ni(2)–N(4) = 2.095(4) Å and Ni(2)–O(4) = 2.073(3) Å, with the bond angle N(4)–Ni(2)–O(4) = 164.64(13)°. The bond distances and angles around the two nickel(II) centers are very similar. The nickel–nickel separation bridged by the two phenolic oxygen atoms is 3.1605(8) Å with Ni–O–Ni angles of 99.36 and 99.93(13)°.

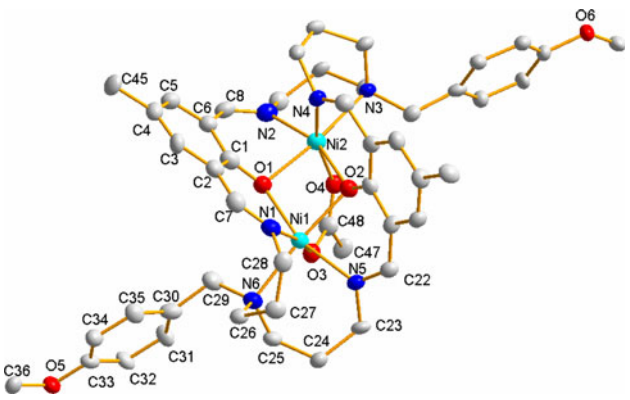

Fig. 1 Perspective view of the complex. Hydrogen atoms and counter-ion are omitted for clarity (ellipsoids are drawn at 30% probability)

Table 1 Crystal data and details of the structure determination for the complex

Empirical	$C_{48}H_{61}ClN_6Ni_2O_{11}$
Formula weight	1,050.90
Crystal system	Monoclinic
Space group	P 21
a, Å	17.110(3)
b, Å	17.618(2)
c, Å	18.163(3)
α, °	90.00
β, °	99.349(3)
γ, °	90.00
Volume (Å^3)	5402.6(15)
Z	4
D (calc) (g/cm^3)	1.292
Mu (Mokα) [/nm]	0.806
F(000)	2,208
Crystal size [mm]	0.20 × 0.22 × 0.26
Temp., K	291
Mo Kα radiation (Å^3)	0.71073
Range (deg)	2.1, 26.0
Nref, Npar	10,594, 636
Tot., uniq. data *R*(int)	30,606, 10,594, 0.043
Observed data [$I > 2.0$sigma(I)]	5,325
R, wR_2, S	0.0501, 0.1670, 1.09
Min. and Max. Resd. Dens.[e/Å^3]	−0.54, 0.59

Spectroscopic analysis of DNA-binding activity

Electronic absorption spectroscopy is one of the most useful methods for DNA-binding studies of metal complexes. Intercalative binding of a complex to DNA generally results in hypochromism along with a red shift of the band [21]. The absorption spectra of the nickel complex in the absence and presence of CT-DNA at different concentrations (0–150 μM) are given in Fig. 2. The spectrum of the Ni(II) complex shows a very strong absorption at 395 nm, which is attributed to a metal-to-ligand charge transfer (MLCT) [22, 23]. The band shows a bathochromic shift of about 38 nm and hypochromism of 23.4% after adding DNA. These findings support the hypothesis of a DNA intercalating interaction of the complex [24]. The value of K_b was obtained from the ratio of slope to the intercept from the plot of $[DNA]/(\varepsilon_a - \varepsilon_f)$ versus [DNA] (Fig. 3). The K_b value is 2.6×10^4 M^{-1}. Comparing the intrinsic binding constant of this Ni(II) complex with those of DNA-intercalative macrocyclic Cu(II) complexes [7],

Table 2 Selected bond distances (Å) and angles (°) for nickel complex

Bond	Distance	Bond	Distance
N1–Ni1	2.115(4)	N2–Ni2	2.073(4)
N5–Ni1	2.081(4)	N3–Ni2	2.232(4)
N6–Ni1	2.223(4)	N4–Ni2	2.095(4)
Ni1–O1	2.053(3)	Ni2–O2	2.053(3)
Ni1–O3	2.069(3)	Ni2–O4	2.073(3)
Ni1–O2	2.075(3)	Ni2–O1	2.092(3)
Bond	**Angle**	**Bond**	**Angle**
O1–Ni1–O3	86.14(12)	O2–Ni2–N2	159.50(15)
O1–Ni1–O2	77.76(12)	O2–Ni2–O4	85.73(12)
O3–Ni1–O2	90.91(12)	N2–Ni2–O4	88.31(14)
O1–Ni1–N5	160.12(14)	O2–Ni2–O1	77.37(12)
O3–Ni1–N5	87.04(13)	N2–Ni2–O1	83.25(15)
O2–Ni1–N5	83.70(13)	O4–Ni2–O1	91.87(12)
O1–Ni1–N1	86.11(14)	O2–Ni2–N4	85.83(13)
O3–Ni1–N1	166.26(14)	N2–Ni2–N4	103.85(15)
O2–Ni1–N1	98.52(13)	O4–Ni2–N4	164.64(13)
N5–Ni1–N1	103.84(15)	O1–Ni2–N4	98.78(13)
O1–Ni1–N6	107.63(13)	O2–Ni2–N3	109.58(12)
O3–Ni1–N6	88.64(13)	N2–Ni2–N3	89.90(15)
O2–Ni1–N6	174.54(13)	O4–Ni2–N3	89.18(12)
N5–Ni1–N6	90.84(14)	O1–Ni2–N3	173.03(12)
N1–Ni1–N6	82.92(14)	N4–Ni2–N3	81.60(13)

we can deduce that the Ni(II) complex binds to DNA by moderate intercalation.

It is well known that mixed solutions of DNA and EB show very strongly enhanced fluorescence emission [25] due to intercalation of EB to DNA. In our experiments, when the Ni(II) complex was added to the EB-DNA system, the emission intensity was reduced. The emission spectra of EB bound to DNA in the absence and presence of the complex are given in Fig. 4. The significant reduction in fluorescence intensity of the EB-DNA solution on addition of the complex suggests that the Ni(II) complex can displace the EB and therefore bind to the DNA.

The binding of the complex to DNA can be determined according to the classical Stern–Volmer equation (2):

$$I_0/I = 1 + K[Q] \quad (2)$$

In which, I_0 and I are the fluorescence intensities of EB-DNA in the absence and presence of complex, respectively. K is the linear Stern–Volmer quenching constant, and $[Q]$ is the concentration of the complex [26]. The fluorescence intensity at 605 nm ($\lambda_{ex} = 520$ nm) of EB in the bound form was plotted against the compound concentration. The quenching constant K obtained for the complex is

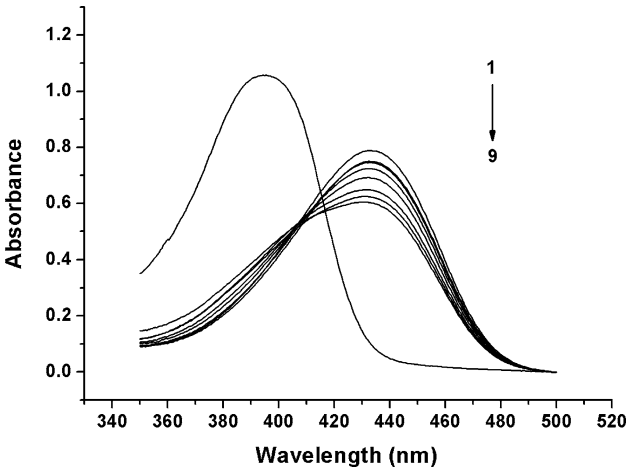

Fig. 2 UV-visible spectra of the Ni(II) complex in the presence of increasing amounts of CT-DNA in 50 mM Tris–50 mM NaCl aqueous buffer solution (pH = 7.2). [M] = 50 μM, [DNA] = 0 (*1*), 4.4 (*2*), 9 (*3*), 13 (*4*), 19 (*5*), 25 (*6*), 37 (*7*), 72 (*8*), 150 (*9*) μM

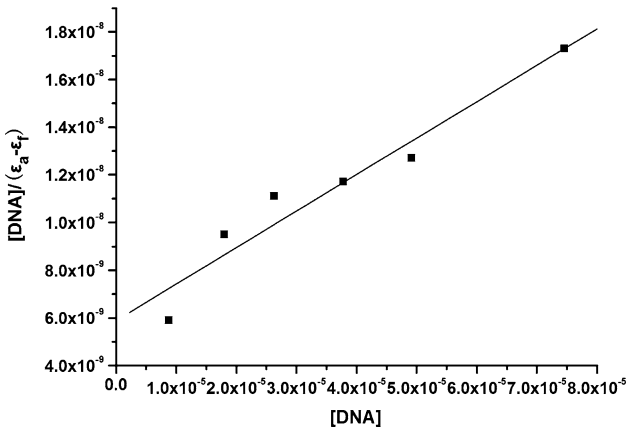

Fig. 3 Plot of $[DNA]/(\varepsilon_a - \varepsilon_f)$ versus [DNA] for absorption titration of CT-DNA with the complex

given by the slope of the plot in Fig. 5, as 7.57×10^3 M^{-1}. The constant is smaller than those of DNA-intercalative complexes [6, 24], so we deduce that the Ni(II) complex binds to DNA with a moderate intercalative mode.

We have also investigated the DNA binding of the complex by circular dichroism spectroscopy. CT-DNA is normally present in the B-DNA form and shows a negative CD band at 245 nm caused by the helical conformation and a positive CD band at 275 nm due to base stacking [27]. The CD spectra of CT-DNA treated with the Ni(II) complex with a ratio of 0.5 ([complex]/[DNA]) show an evident disturbance on the CT-DNA conformation. Both positive and negative bands increased in intensity when the complex was added to the CT-DNA solution, with more evident changes for the negative band (Fig. 6). These data suggest that the complex can intercalate the DNA and unwind the DNA helix [28].

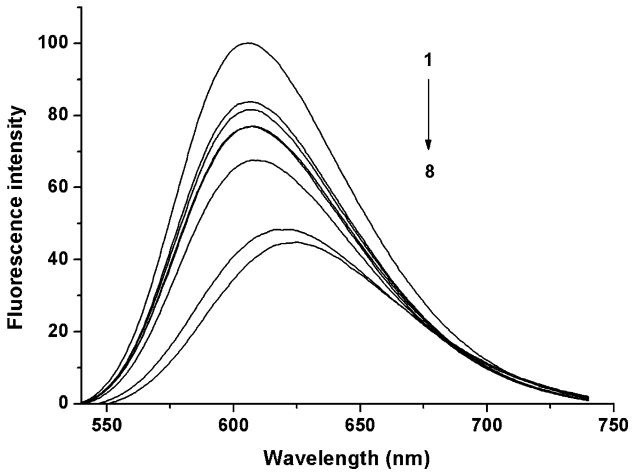

Fig. 4 Emission spectra of EB bound to DNA in the absence (*1*) and presence (*2–8*) of the complex. [EB] = 10 μM, [DNA] = 25 μM, [complex] 1–8 = 0, 12.5, 25, 30, 50, 100, 160, 200 μM, respectively; λ_{ex} = 520 nm. The *arrow* shows the intensity changes on increasing the complex concentration

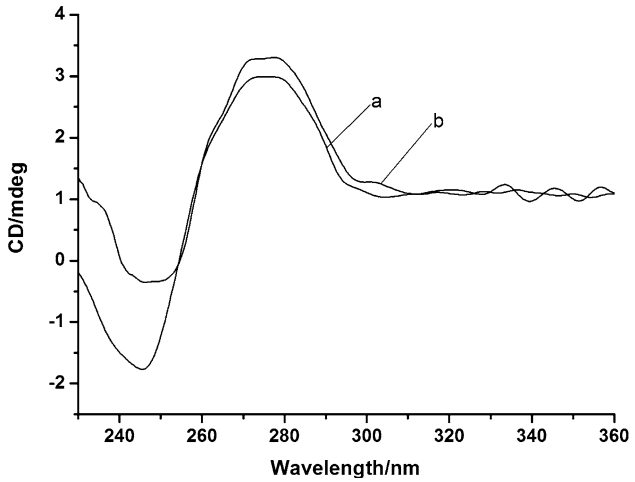

Fig. 6 The circular dichromism spectra of CT-DNA in the absence (*a*) and presence of the complex (*b*). [CT-DNA] = 25 μM, [complex]/[DNA] = 0.5. All the spectra were recorded in Tris–HCl buffer, pH = 7.2

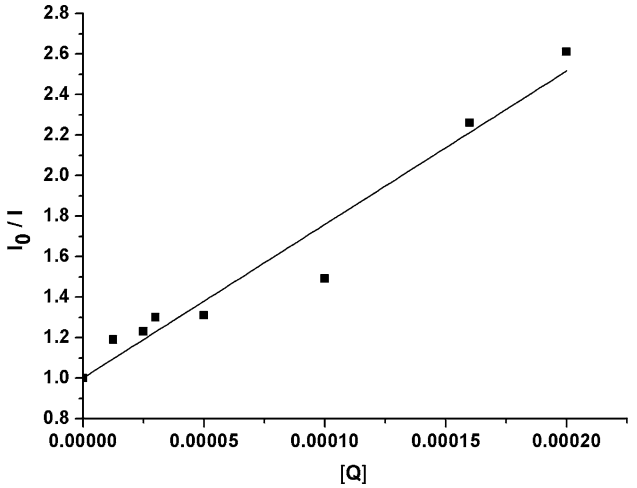

Fig. 5 Stern–Volmer quenching plot of EB bound to DNA by Ni(II) complex. I_0 is the emission intensity of EB-DNA in the absence of complex; I is emission intensity of EB-DNA in the presence of complex; [Q] = [complex]

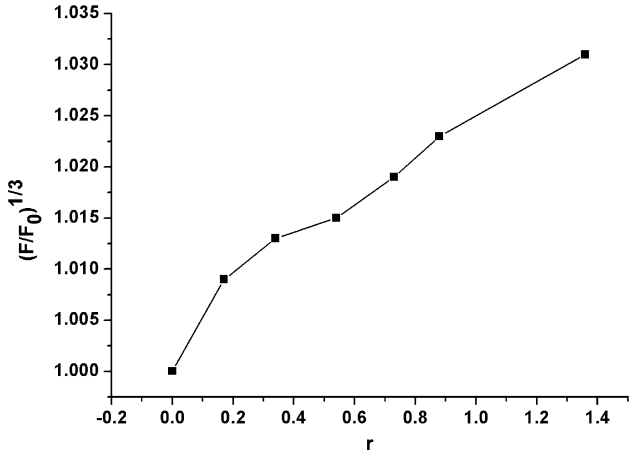

Fig. 7 Effects of increasing amounts of the complex on the relative viscosities of CT-DNA at 23.0 (±0.1) °C; [DNA] = 147 μM, r = [M]/[DNA]

Viscosity and electrochemical studies

To further confirm the interaction mode of the Ni(II) complex with DNA, a viscosity study was carried out (Fig. 7). The specific viscosity of the DNA increases obviously with increased concentration of the complex. This again suggests that the binding mode between the complex and DNA may be intercalation [29, 30].

The electrochemical properties of the complex were studied by cyclic voltammetry in 50 mM Tris–HCl/50 mM NaCl buffer solution (pH = 7.2) using tetrabutyl ammonium perchlorate (TBAP) as supporting electrolyte and a sweep range of −1.0 to −0.4 V. The cyclic voltammograms of the complex in the absence and in the presence of CT-DNA are shown in Fig. 8. In the absence of DNA, the CV curve of the complex has a cathodic peak at −0.596 V and an anodic peak at −0.840 V. The separation between the cathodic and anodic peak potential, ΔE = 0.244 V, indicates a quasi-reversible process [31]. Addition of CT-DNA to the Ni(II) complex results in a decrease in the cathodic and anodic peak current, which could be explained by a reduction in the apparent diffusion coefficient of the complex on binding to DNA [32]. These results again indicate that an intercalative interaction occurred between the complex and DNA [33].

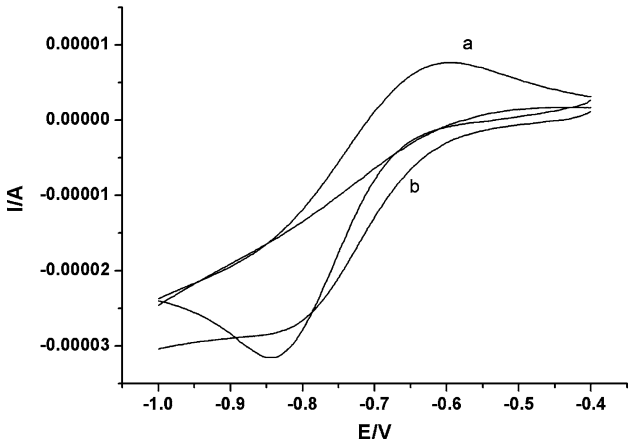

Fig. 8 Cyclic voltammograms of the complex (5×10^{-4} M) in the absence (*a*) and presence (*b*) of CT-DNA (5×10^{-4} M) in 50 mM Tris–HCl/50 mM NaCl buffer solution (pH = 7.2), scan rate: 0.1 V/s

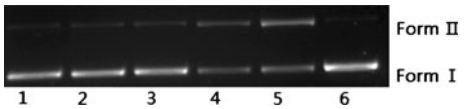

Fig. 9 Agarose gel electrophoresis of pBR322 plasmid DNA in the presence of different concentrations of the complex. DNA (0.5 μL) with complex (1 μL) was incubated for 3 h in Tris–HCl buffer (1 μL, 50 mM Tris–50 mM NaCl, pH = 7.2) at 37 °C. *Lane 6* DNA control; *Lanes 1–5* DNA + Ni(II) complex (6.25, 12.5, 25, 50, 100 μM)

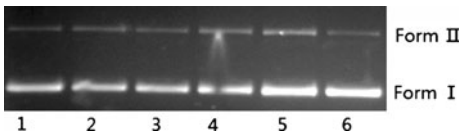

Fig. 10 Time dependence of the cleavage of DNA (0.5 μL) with the complex (1 μL, 100 μM) after incubation at 37 °C in Tris–HCl (1 μL, 50 mM Tris–50 mM NaCl, pH = 7.2) buffer solution. *Lane 6* DNA control; *Lanes 1–5* reaction times of 1, 1.5, 2, 2.5, and 3 h, respectively

DNA cleavage

The cleavage of supercoiled plasmid pBR322 DNA by the complex was studied in the absence of H_2O_2 or any reducing agents. As shown in Fig. 9, with increasing concentrations of the complex, the amount of Form I (supercoiled form) of DNA diminished obviously, whereas Form II (nicked form) increased. This suggests that the complex can cleave the DNA effectively, but the cleavage efficiency is lower than that of a non-macrocyclic Ni(II) complex described in the literature [34].

Figure 10 shows the time dependence of the cleavage reactions of DNA with the Ni(II) complex after incubation (pH = 7.2, 37 °C). With increasing incubation time, the cleavage of DNA increased obviously.

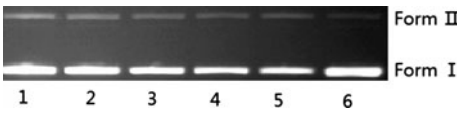

Fig. 11 Agarose gel showing cleavage of pBR322 DNA (0.5 μL) incubated with the complex (1 μL, 100 μM) in Tris–HCl buffer (1 μL, 50 mM Tris–50 mM NaCl, pH = 7.2) at 37 °C for 3 h. *Lane 6* DNA control; *Lanes 1–5* DNA + complex + EtOH, DNA + complex + DMSO, DNA + complex + KI, DNA + complex + NaN_3, DNA + complex

In order to further clarify the DNA cleavage mechanism, cleavage trials were carried out in the presence of typical scavengers [35] for singlet oxygen (NaN_3, 3 mM), for superoxide (KI, 3 mM), and for hydroxyl radical (DMSO, 1 mM and EtOH, 1 mM). As shown in Fig. 11, there is no evidence of inhibition on the DNA cleavage in the presence of all these scavengers. Therefore, DNA cleavage promoted by this complex might not occur by an oxidative pathway but rather by a hydrolytic pathway.

Conclusion

In conclusion, a macrocyclic Ni(II) complex has been synthesized and structurally characterized. The biological activities of the complex toward calf thymus DNA were studied by UV absorption, fluorescence spectroscopy, CD spectra, viscosity, and electrochemistry. The binding constant of the complex with CT-DNA is 2.6×10^4 M^{-1}, and the linear Stern–Volmer quenching constant calculated from fluorescence experiments is 7.57×10^3 M^{-1}. The results indicate that this complex binds to DNA by a moderate intercalation mode. Moreover, the Ni(II) complex shows an efficient cleavage activity toward supercoiled DNA (pBR322 DNA) in the absence of any external agents. We propose the DNA cleavage promoted by this complex occurs via a hydrolytic pathway.

Supplementary material

Crystallographic data have been deposited with the Cambridge Crystallographic Data Center, under deposition number CCDC 803850 for the complex $[Ni_2(OAc)L]ClO_4{\cdot}H_2O$. Copy of the data can be obtained free of charge on application to The Director, CCDC, 12 Union Road, Cambridge CB2, 1EZ, UK (fax: +44-1223-336033); E-mail: deposit@ccdc.cam.ac.uk or http://www.ccdc.cam.ac.uk).

Acknowledgments This work was supported by National Nature Science Foundation of China (No. 20971102, 21002076), the foundation for midlife and youth excellent innovation group of Hubei Province, China (No. T200802), the key foundation of the Education Department of Hubei Province, China (No. D20081503).

References

1. Chen ZF, Wang XY, Li YZ, Guo ZJ (2008) Inorg Chem Conmun 11:1392–1396
2. Sheng X, Guo X, Lu XM, Lu GY, Shao Y, Liu F, Xu Q (2008) Bioconjugate Chem 19:490
3. Maheswari PU, Roy S, Dulk HD, Barends S, Wezel GV, Reedijk J (2006) J Am Chem Soc 128:710
4. Chin J, Banaszczyk M, Jubian V, Zou X (1989) J Am Chem Soc 111:186
5. Lu ZL, Liu CT, Neverov AA, Brown RS (2007) J Am Chem Soc 129:11642
6. Qian J, Gu W, Liu H, Gao FX, Feng L, Yan SP, Liao DZ, Cheng P (2007) Dalton Trans 177:1060–1066
7. Anbu S, Kandaswamy M, Suthakaran P, Murugan V, Varghese B (2009) J Inorg Biochem 103:401–410
8. Kong DM, Wang J, Zhu LN, Jin YW, Li XZ, Shen HX, Mi HF (2008) J Inorg Biochem 102:824–832
9. Gagne RR, Spiro CL, Smith TJ, Hamann CA, Thies WR, Shiemke AK (1981) J Am Chem Soc 103:4081
10. Gerard PM, David PK, Mack P (2001) Molecules 6:234–242
11. Zeng QD, Qian M, Gou SH, Fun HK, Duan CY, You XZ (1999) Inorg Chim Acta 294:2
12. Smart and Saint (1996) Area detector control and integration software. Siemens Analytical X-Ray Systems Inc., Madison
13. Sheldrick GM (1997) SHELXTL V5.1 software reference manual. Bruker AXS Inc., Madison
14. Reichmann ME, Rice SA, Thomas CA, Doty P (1954) J Am Chem Soc 76:3047–3053
15. Pyle AM, Rehmann JP, Meshoyrer R, Kumar CV, Turro NJ, Barton JK (1989) J Am Chem Soc 111:3055–3056
16. Ivanov VI, Minchenkova LE, Schyolkina AK, Poletayev AI (1973) Biopolymers 12:89–110
17. Cohen G, Eisenberg H (1969) Biopolymers 8:45–49
18. Sellamuthu A, Muthusamy K, Babu V (2010) Dalton Trans 39: 3824–3825
19. Zhou H, Peng ZH, Pan ZQ, Song Y, Huang QM, Hu XL (2007) Polyhedron 26:3235–3238
20. Liang SL, Liu ZL, Liu NR, Liu CM, Di XW, Zhang J (2010) J Coord Chem 63(19):3444–3445
21. Barton JK, Danishefsky AT, Goldberg JM (1984) J Am Chem Soc 106:2172–2176
22. Neves A, de Brito MA, Vencato I, Drago V, Griesar K, Haase W (1996) Inorg Chem 35:2360
23. Gaber BP, Miskowski V, Spiro TG (1974) J Am Chem Soc 96:6868
24. Tian JL, Feng L, Gu W, Xu GJ, Yan SP, Liao DZ, Jiang ZH, Cheng P (2007) J Inorg Biochem 101:199–200
25. Meyer-Almes FJ, Porschke D (1993) Biochemistry 32:4246–4253
26. LePecq JB, Paoletti C (1967) J Mol Biol 27:87–106
27. Maheswari PU, Palaniandavar M (2004) J Inorg Biochem 98:219–230
28. Shao Y, Sheng X, Li Y, Jia ZL, Zhang JJ, Liu F, Lu GY (2008) Bioconjugate Chem 19(9):1842–1843
29. Sun J, Shuo S, An Y, Liu J, Gao F, Ji LN, Mao ZW (2008) Polyhedron 27:2846
30. Liu JG, Ye BH, Li H, Zhen QX, Ji LN, Fu YH (1999) J Inorg Biochem 76:266
31. Zhang JA, Pan M, Yang R, She ZG, Kaim W, Fan ZJ, Su CY (2010) Polyhedron 29:590–591
32. Ibrahim MS (2001) Anal Chim Acta 443:65–71
33. Michael TC, Marisol R, Alle JB (1989) J Am Chem Sol 111(24):8901–8911
34. Song YM, Wu Q, Yang PJ, Luan NN, Wang LF, Liu YM (2006) J Inorg Biochem 100:1687–1688
35. An Y, Tong ML, Ji LN, Mao ZW (2006) Dalton Trans 2069–2070